Time-dependent spectroscopic observation of the magnetic field in a high-power-diode plasma

Y. Maron, E. Sarid, E. Nahshoni, and O. Zahavi
Department of Physics, Weizmann Institute of Science, Rehovot 76 100 Israel
(Received 27 January 1988; revised manuscript received 26 January 1989)

The magnetic field in the anode plasma of a magnetically insulated ion-beam diode has been measured as a function of time by the observation of Zeeman splitting of line emission. With use of this technique, the plasma was found to be penetrated by the magnetic field applied in the diode early in the pulse. The diamagnetic effect of the electron flow in the diode acceleration gap was found to be much larger than that calculated from one-dimensional solutions for the magnetically insulated gap. However, it agrees with the measured ion current density and the observed electric field distributions across the diode gap that showed significant electron flow beyond the calculated electron-sheath region. The penetration of the diamagnetic signal into the plasma indicates an anomalous plasma conductivity that is at least ten times lower than the classical conductivity.

I. INTRODUCTION

In pulsed electrically stressed devices plasmas are either generated over surfaces in the devices due to the strong electric fields and the large currents or are supplied there by external means. Also in such devices, magnetic fields may be externally applied or can be produced by the currents flowing in the device. The presence (or absence) of magnetic fields in the plasmas significantly affects the current flow, the resultant plasma heating, the plasma motion, and the thermal convection and thus plays an important role in the overall operation of the devices.

Examples of such devices are electron-beam diodes,[1] ion diodes,[2,3] high-power magnetrons,[4] magnetically insulated transmission lines,[5] and high-power plasma switches.[6,7] For plasmas that serve as ion sources, the presence of the magnetic field in the plasma is expected to influence the flow of various ionic species and thus to affect the composition of the extracted ion beams. Finally, knowledge of the time-dependent diamagnetic effects in the plasma of a pulsed device provides information about the time-dependent current flow in the device.

A common way to measure magnetic fields in these devices is to use magnetic loops. The insertion of such loops in plasmas usually produces a disturbance and in high-voltage devices may cause wiring problems. In high-power diodes the use of magnetic loops is especially difficult, and often impossible, due to the large currents, the strong electric fields, and the smallness of the diode gap. In addition, measurements by magnetic loops usually suffer from pickup noise.

Here, we report on time-dependent measurements of the magnetic field in the anode plasma of a magnetically insulated ion-beam diode by the observation of Zeeman splitting of spontaneous line emission from Ba II ions in the plasma. The magnetic field applied in the diode was found to be present in the plasma a few nanoseconds after the plasma appeared and throughout the entire pulse. The time-dependent diamagnetic effect due to the electron flow in the diode gap was also seen. The rise in the magnetic field on the anode side was found to be much larger than that obtained from a one-dimensional Brillouin-flow model calculation.[8] However, it is consistent with estimates[9] based on the measured ion current density and on the electric field distribution across the diode acceleration gap observed[10] for a similar diode configuration. Those observations showed significant electron flow close to the anode plasma, beyond the calculated[8] electron-sheath region, which should enhance the diamagnetic effect on the anode side. The penetration into the anode plasma of the diamagnetic signal due to the electron flow in the gap was found to be in disagreement with calculations based on a classical plasma conductivity. It was rather consistent with an anomalous plasma conductivity that is at least ten times lower than the classical conductivity. This anomalous conductivity also explains the relatively fast plasma expansion against the magnetic field[11] and the uniformity of the electron temperature in the plasma.[12] Furthermore, together with the pressure-driven current in the plasma, it also yields a reasonable Ohmic heating rate for the plasma electrons.[12]

II. EXPERIMENTAL ARRANGEMENT

For the present experiments we used a planar magnetically insulated diode, as described in Ref. 11. The insulating magnetic field B_z which inhibits the electron flow across the 8-mm-wide diode gap was varied in the experiments between 4 and 8 kG.

The anode plasma was formed as a result of a surface flashover of the epoxy-filled grooved aluminum anode. The height in the y direction of the active anode was 6 cm and its length in the z direction was 14 cm. The diode was powered by a 270-kV, 90-ns pulse delivered by an LC generator coupled to a 1 Ω water line. The use of a low-impedance line was advantageous for our experiments since it allowed the voltage pulse height on the relatively

high-impedance (usually $>10\ \Omega$) diode to be almost independent of the applied magnetic field.

Light was collected from the anode plasma parallel to the magnetic-field lines. The measurements integrated along the active anode length and along the 3.5-cm-high central part of the anode. The spatial resolution in the gap direction (the x direction) was <0.1 mm (see Sec. III).

In order to observe Zeeman splitting of a fraction of an angstrom (corresponding to our 4–8-kG magnetic fields) a spectral resolution of 0.1 Å is required. This was obtained by using optical magnification at the spectrograph output and a fiber-photomultiplier tube system. This system yielded 11 points of the spectral line profile as a function of time, with a temporal resolution of 5 ns, in a single discharge. Other details of the diode arrangement and the diagnostic system are given in Ref. 11.

III. MEASUREMENTS AND RESULTS

As discussed in Ref. 11, line emission from the anode plasma first appears at $t=t_0\simeq 20$ ns after the start of the diode voltage pulse. At $t\simeq 50$ ns the plasma is seen to occupy an about 1.5-mm-wide region near the anode surface. Later on in the pulse, the plasma expands into the diode gap with a velocity of about 1 cm/μs. The average plasma electron density and temperature were observed to be approximately 2.2×10^{15} cm^{-3} (Ref. 11) and 5–8 eV.[12] The magnetic field is measured only for $t\gtrsim 25$ ns, when sufficient line emission occurs.

Since the line emission is collected parallel to the magnetic field lines, only the $\Delta M=\pm 1$ line components are observed. These components are divided into two groups shifted in opposite directions with respect to the line center. The spectral shift of each component relative to the line center is given by

$$\Delta\omega=\frac{\mu_0 B}{\hbar}[g_u M-g_l(M\pm 1)]\ , \tag{1}$$

where $\mu_0=e\hbar/2mc$, m is the electron mass, B is the magnetic field, and g_u and g_l are the g factors of the upper and lower levels, respectively.

In order to obtain the magnetic field from the spectral line profile, the Zeeman splitting must dominate over other contributions to the line profile. The main broadening mechanism of the line emission from our anode plasma is the Doppler broadening, due to the ion kinetic energies observed to be $\gtrsim 20$ eV,[11] which amounts to a fraction of an angstrom in the visible range. Since the ion velocities in the plasma were found to be smaller for heavier ions the Doppler-broadening effect can be reduced by using line emission from heavy ions. In addition, the use of longer wavelengths is preferable due to the relative increase of the Zeeman splitting (over the Doppler broadening) with the wavelength.

For our measurements we used lines of Ba II ions that were added to the anode plasma by mixing the epoxy used for the anode with 60% by weight of BaF_2 powder. An upper limit on the Ba II ion velocities was obtained from the spectral profile of the Ba II 2634-Å line shown in Fig. 1(b), which is similar to the system spectral resolution curve given in Fig. 1(a). Since with the present spectral resolution line Doppler broadening of about 0.1 Å would have been noticeable, we conclude that an upper limit for the Ba II kinetic energy is 30 eV. This is consistent with the velocity distributions observed for the singly charged ions in the plasma (C II, Mg II, Si II, and Ca II). These distributions were found to be Gaussian-like, corresponding to mean kinetic energies between 20 and 40 eV.[11]

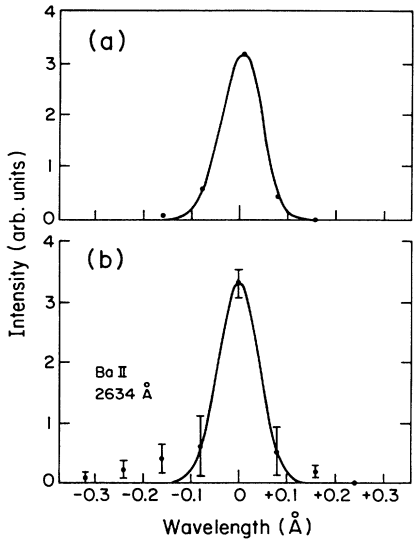

FIG. 1. (a) Measurement of the system spectral resolution using the 2536-Å line of a low-pressure Hg lamp. (b) Spectral line profile of the Ba II 2634-Å line. The curves are Gaussian fits to the data.

An additional advantage of using Ba II ions (except for the small Doppler broadening) was that these ions remain close to the anode surface throughout the entire pulse. This results from the low velocity and the fast ionization of Ba II. Using collisional-radiative calculations,[13] based on the observed plasma electron density and temperature, the Ba II ions are estimated to ionize in less than 10 ns. Therefore, the Ba II ions can move less than 0.1 mm from the anode surface before they ionize. This was verified by measuring the axial intensity distribution of the Ba II 4554-Å line. In these measurements the spatial resolution in the x direction of the spectroscopic system was $\simeq 0.11$ mm. This was obtained by using an f number of 34, a demagnification factor of 5.3 for the lens L, and a relatively short anode (2 cm long) in the z direction to reduce the effect of defocusing along the line of sight. The measured intensity distribution at the end of the pulse is shown in Fig. 2. Also shown is the actual distribution derived from the measured distribution by deconvolution using the known spatial resolution. The actual Ba II line-intensity drops considerably within 0.1 mm from the anode surface. This enabled us to measure the magnetic field very close to the anode surface with a spatial resolution less than 0.1 mm independent of the light collection optics, thus allowing for efficient light collection.

An example of a Zeeman-split Ba II line, the 6142-Å

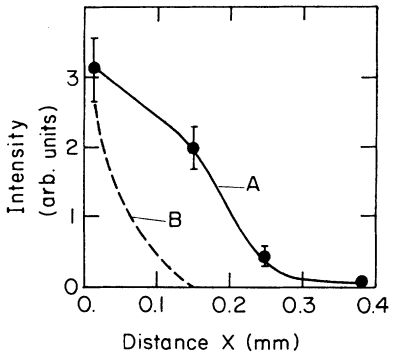

FIG. 2. Measured intensity of the Ba II 4554-Å line as a function of distance x from the anode surface for $t=95$ ns after the start of the diode voltage pulse. The data points are connected by a smooth curve (curve A). The error bars shown result from the shot-to-shot irreproducibility. Also shown is the intensity distribution (curve B) deconvolved from the measured distribution using the system spatial resolution in the x direction determined by scanning a narrow light source.

line, is shown in Fig. 3(a). The errors in the data points result from the uncertainty in the synchronization of the photomultiplier-tube traces (overestimated to be ± 5 ns) and the uncertainty in the relative photomultiplier-tube calibration. The spectral profile given in Fig. 3(a) shows the line splitting into two main groups, as anticipated. In order to determine the magnetic field from the measured spectral line profile we use the calculated line splitting [given in Eq. (1)] and relative component intensities parallel to the magnetic field. In the case of the Ba II 6142-Å line, each side group consists of four components,

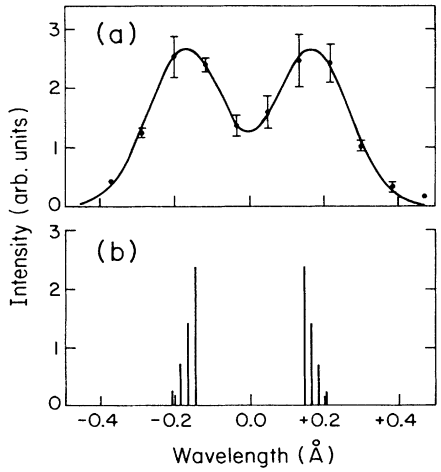

FIG. 3. (a) Spectral profile of the Ba II 6142-Å line observed with an applied magnetic field $B_{app}=7.6$ kG. The uncertainty in the data points is less than $\pm 15\%$. The curve is a best fit of convolution of Gaussian profiles assumed for each of the emission components shown in (b). (b) the Zeeman-split emission pattern of the Ba II $5d\,^2D_{5/2}-6p\,^2P_{3/2}$ transition (the 6142-Å line).

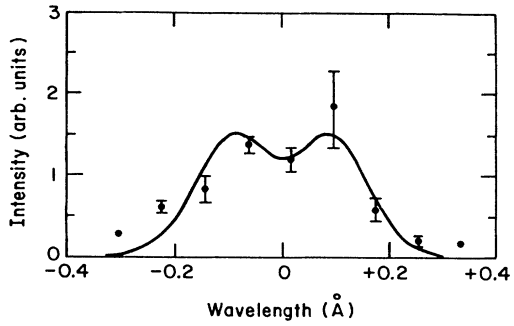

FIG. 4. Spectral profile of the Ba II 4554-Å line observed with an applied magnetic field $B_{app}=6.0$ kG. The curve is a best fit of convoluted Gaussian profiles for the emission components.

as shown in Fig. 3(b). In the present measurements these components are unresolved due to the Doppler broadening. A Gaussian spectral profile (that accounts for the Doppler broadening and the instrumental spectral resolution) is assumed for each component. The magnetic field is then obtained from a best fit of the computed emission pattern to the data points, optimized over the Doppler broadening and the magnetic field. Such a best fit is shown in Fig. 3(a). The best fits were always obtained for Doppler broadening well within the uncertainty range of the kinetic energy (up to 30 eV), and the inferred magnetic field was not sensitive to the uncertainty in the Doppler broadening. The best fit to the data in Fig. 3(a) gives $B=8.3\pm 0.3$ kG. Besides this uncertainty, there is an uncertainty of $\pm 6\%$ in the absolute value of B, common to all results reported here, caused by the uncertainty in the spectral widths of the fiber channels.

The Zeeman splitting of another Ba II line, the 4554-Å

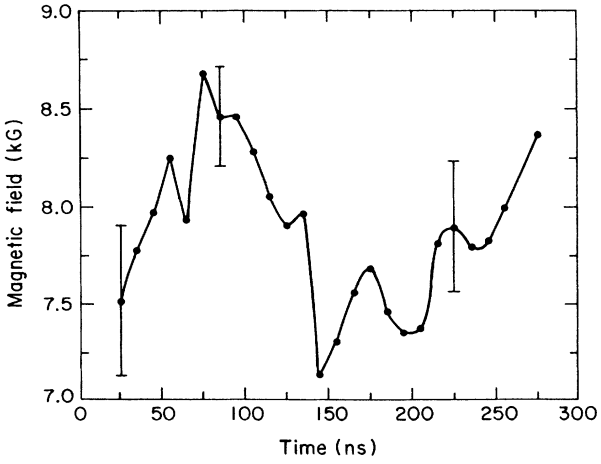

FIG. 5. Magnetic field as a function of time, observed using the Ba II 6142-Å line, for $B_{app}=7.6$ kG. The absolute uncertainty in B_{app} and in the observed magnetic field is $\pm 10\%$ and $\pm 6\%$, respectively.

line, was also observed. However, these measurements are less accurate because of the smaller splitting as shown by the spectral profile given in Fig. 4. The uncertainty in B in these measurements was $\pm 10\%$ and the magnetic field inferred agreed with that obtained from the 6142-Å line to within this uncertainty.

A typical measurement of the magnetic field as a function of time near the anode surface, obtained for an applied magnetic field $B_{app}=7.6$ kG using the Ba II 6142-Å line, is shown in Fig. 5. The uncertainty of about $\pm 5\%$ depends, for each instant of time, on the line intensity, the rate of the intensity change, and the line splitting. It is seen that the magnetic field is present in the plasma already at $t=25$ ns and then remains in the plasma throughout the pulse. Repeated measurements gave similar results. The temporal variation of the magnetic field during and after the pulse ($t>100$ ns) will be discussed below.

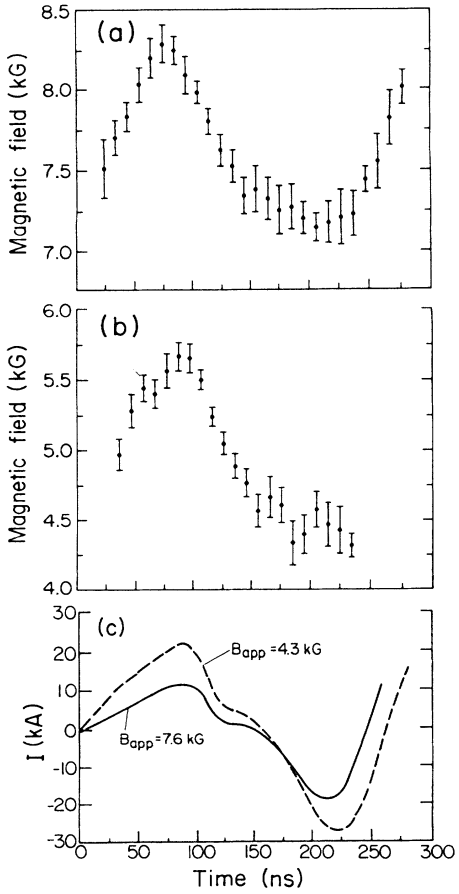

FIG. 6. (a) Magnetic field as a function of time, observed using the Ba II 6142-Å line, for $B_{app}=7.6$ kG. The data points are averaged over $N=11$ identical discharges. The error bars shown for each time are the standard deviations divided by $\sqrt{N-1}$. Besides these error bars shown there is an uncertainty of $\pm 6\%$ in the absolute value of the observed magnetic field. The uncertainty in B_{app} is $\pm 10\%$. (b) The same as (a) for $B_{app}=4.3$ kG and $N=13$ discharges. (c) Total diode current wave forms for the two fields.

As stated in Sec. I, measurements of the time-dependent magnetic field in the anode plasma can give the diamagnetic effects on the anode side of the electron $E\times B$ drift parallel to the anode in the diode acceleration gap. This electron drift tends to increase the magnetic field on the anode side and to reduce it on the cathode side. However, for our low current diode ($\lesssim 20$ kA) the diamagnetic effects are too small to be clearly seen beyond the uncertainty in a single discharge. In order to reliably determine the diamagnetic effect, we averaged the results of N identical measurements, thus reducing the uncertainty by the factor $\sqrt{N-1}$ (due to the randomness of the relative uncertainty in the magnetic-field determination).

We observed the time-dependent magnetic field in the plasma for $B_{app}=7.6$ and 4.3 kG using $N=11$ and 13 discharges, respectively, as shown in Figs. 6(a) and 6(b). The waveforms of the total diode current, given in Fig. 6(c), were similar for the two magnetic fields with the current peaking at 13 and 21 kA, respectively. To within the uncertainties the magnetic field in the anode plasma at early times equals the applied magnetic field as mentioned above. The field then rises and drops during the current pulse. This demonstrates the diamagnetic effects due to the current flow in the diode acceleration gap. For $B_{app}=7.6$ kG [Fig. 6(a)] the magnetic field rises by about 0.8 kG during the pulse, then drops to about the applied field when the diode current I is zero ($t\simeq 150$ ns), followed by a decrease below B_{app} when $I<0$. The magnetic field rises again above B_{app} when I rises ($t\gtrsim 250$ ns). For $B_{app}=4.3$ kG [Fig. 6(b)], the peak diamagnetic signal during the pulse is about 1.2 kG. Also in this case the observed magnetic field drops to about B_{app} when I decreases to about zero.

IV. DISCUSSION

The formation and the expansion of the anode plasma during the first 20 ns of the pulse have not as yet been investigated experimentally. Recently, Litwin and Maron[14] suggested a mechanism for the early plasma production within this region, based on the formation of an expanding neutral layer and the subsequent ionization of this layer by electron avalanche. This model led to plasma density and thickness consistent with those observed early in the pulse ($\simeq 2\times 10^{15}$ cm^{-3} and $\simeq 1.5$ mm, respectively).[11] The formation of the plasma due to ionization of a neutral layer formed early in the pulse is consistent with the observed presence of the magnetic field in the plasma at this time ($t=25$ *ns*, see Figs. 5 and 6).

The continued presence of the magnetic field in the plasma later on in the pulse can be expected from the plasma conductivity and observed expansion rate ($\simeq 1$ cm/μs).[11] The magnetic Reynolds number, even for a classical conductivity[15] that corresponds to the observed electron temperature of $\simeq 7$ eV,[12] is about 0.2.

The presence of the magnetic field in the plasma causes currents in the $-y$ direction due to the pressure gradients in the plasma. This current density $j_y=c\partial_x P/B$ (where c is the speed of light and $\partial_x P$ is the x derivative of the plasma pressure) was estimated using the observed ion

temperature, electron temperature, and plasma density to be $\simeq -1600$ A/cm^2.[11] This current may have an important effect on the plasma behavior since the associated electron drift may make the plasma unstable.[11] It is also probably responsible for the electron heating in the plasma.[12]

Knowledge of the magnetic field in the plasma also enables us to estimate the magnetization and the thermal convection of the electrons. The electrons are magnetized since $\omega_{ce}/\nu_{ei} \approx 40$ (where ω_{ce} and ν_{ei} are the electron cyclotron frequency and electron proton collision frequency for $T_e = 7$ eV, respectively) and the thermal convection time for a classical plasma conductivity[15] is estimated to be about 700 ns, much longer than the pulse length. Together with the Ohmic electron heating estimated using the diamagnetic currents and the pressure-driven currents in the plasma, this convection time allows us to obtain an estimate for the variation of the electron temperature with the distance from the anode surface.[12]

It is interesting to compare the peak diamagnetic effect observed in the anode plasma to that calculated from a one-dimensional Brillouin flow model.[8] The actual diode gap (the distance between the field-excluding anode and cathode plasmas) is not known for the present experiments. However, since the diode was reasonably well magnetically insulated for $B_{\rm app}$ down to 4.3 kG (which corresponds to a critical diode gap[16] of 4.5 mm), and since in a similar experiment[10] the actual diode gap was seen not to change with the magnetic field, we infer that for the present experiments with $B_{\rm app} = 7.6$ kG the actual diode gap was about 4.5 mm. The one-dimensional Brillouin-flow model[8] then gives a diamagnetic rise $\lesssim 0.2$ kG for the magnetic field on the anode side, much less than that observed [see Fig. 6(a)]. The observed large rise in the magnetic field was predicted in Ref. 10 on the basis of measurements of the electric-field distribution across the diode acceleration gap. From those measurements it was inferred that the electrons in the gap flow close to the anode plasma, beyond the theoretical[8] electron-sheath region, and that the total electron current in the diode gap is larger than the calculated value. This should lead to a magnetic field rise on the anode side larger than the calculated value.

In order to estimate the actual diamagnetic effect in our diode we use the pressure balance formula[9] that relates the magnetic field pressure $B_a^2(t)/8\pi$ on the anode side to that on the cathode side, $B_c^2(t)/8\pi$, by

$$\frac{B_a^2(t)}{8\pi} - \frac{B_c^2(t)}{8\pi} = j_i(t)(2m_i V/ze)^{1/2} , \tag{2}$$

where $J_i(t)$, V, m_i, and ze are the ion current density, the diode voltage, the ion mass, and the ion charge. Here, the electron momentum in the diode acceleration gap was neglected, as shown by simulation calculations,[17] and we used the vanishing of the electric field on the anode and the cathode sides as observed.[10]

For evaluating the right-hand side in Eq. (2), we use our ion current density $J_i(t)$ measured using negatively-biased magnetically insulated charge collectors placed 2 or 5 cm from the anode at five locations in the ion beam. During the diode voltage pulse the ion current density averaged over the various measurements could be approximately fitted for the two applied fields (7.6 and 4.3 kG) by $J_i(t) = 80\{(t-t_0)/35 - [(t-t_0)/70]^2\}$, where $J_i(t)$ is in A/cm^2 and $t - t_0$, in nanoseconds, is the time after the plasma is first seen; see Sec. III. The current density rises to 80 A/cm^2 at the end of the pulse, i.e., at $t = t_0 + 70 = 90$ ns. To determine m_i and ze we obtained the fraction of ions heavier than protons in the ion beam by placing a 2-μm-thick polyethylene foil in front of the cups to eliminate the ions other than protons. From such measurements and ion time-of-flight considerations we concluded that on the average, about half of the ion diode current is carried by nonprotonic ions as also discussed in Ref. 13. The nonprotonic ions in the beam can be assumed to be mainly doubly charged carbon ions.[13] Thus, in evaluating the right-hand side of Eq. (2), we assumed that the beam current contains equal fractions of protons and C III ions.

The exact rise in the magnetic field on the anode side $B_a(t) - B_{\rm app}$ can be determined if the electron current distribution or the electric-field distribution in the gap are known. Using the electric-field distribution observed for a similar diode configuration[10] we estimate that to a good approximation the rise of the magnetic field on the anode side, $B_a(t) - B_{\rm app}$, is similar in magnitude to the field decrease on the cathode side, i.e.,

$$B_a(t) - B_{\rm app} \simeq \tfrac{1}{2}[B_a(t) - B_c(t)] . \tag{3}$$

Using Eqs. (2) and (3) the estimated increase in the magnetic field on the anode side during the pulse is about 0.8 and 1.4 kG for $B_{\rm app} = 7.6$ and 4.3 kG, respectively.

Using the time-dependent magnetic field $B_a(t)$ on the anode side estimated above, we now calculate the penetration of the time-dependent component of the magnetic field into the plasma. We will show that the magnetic field near the anode surface, calculated assuming classical plasma conductivity, is in disagreement with the value observed there.

In order to estimate the magnetic field on the anode surface we assume that at the end of the pulse the plasma is 2 mm thick (this assumption has no effect on our conclusions as will be discussed below). To obtain the magnetic-field distribution across the plasma we assume a uniform semi-infinite plasma at $x \leq 2$ mm, where $x > 2$ mm is the diode acceleration gap. The magnetic field $B_a(t)$ is imposed at $x = 2$ mm. For the solution of the magnetic-field profile in the plasma the assumption that the plasma is semi-infinite is justified since there is a conductor (an aluminum plate) behind the anode-dielectric sheet. Neglecting the displacement current in Ampere's law and assuming a constant plasma conductivity, the equation for the magnetic field $B_z(x,t)$ for a one-dimensional plasma bounded in the x direction (thus allowing no currents in the x direction due to the magnetic field penetration) is

$$\frac{\partial B_z}{\partial t} = D\frac{\partial^2 B_z}{\partial x^2} , \tag{4}$$

where $D = c^2/4\pi\sigma$ is the magnetic diffusion coefficient, c

is the speed of light, and σ is the plasma conductivity. We solve this equation with the initial and boundary conditions $B_z(x,t=t_0)=B_{app}$ and $B_z(x=2,t)=B_a(t)$, respectively. We will return later to the neglect of the convective term in Eq. (4).

We first calculate the magnetic-field distribution assuming a classical plasma conductivity. Assuming, for simplicity, a proton electron plasma, this is given by $\sigma=8.7\times10^{13}T_e^{3/2}/\ln\lambda\ s^{-1}$, where $\ln\lambda$ is the Coulomb logarithm and T_e is in eV.[15] We use a constant electron temperature $T_e=7$ eV. The rise of the magnetic field $\Delta B_z^{cl}(x,t)=B_z(x,t)-B_{app}$ across the plasma, calculated for a classical plasma conductivity, is shown in Fig. 7 for $x=0$ (i.e., 2 mm into the anode plasma) for $B_{app}=7.6$ and 4.3 kG. The uncertainty in $\Delta B_z^{cl}(t)$ results from two factors: (1) The uncertainties in J_i and in the C III fraction in the ion beam, and (2) the uncertainty in the electron temperature (5–8 eV) which affects the classical plasma conductivity. In Figs. 7(a) and 7(b) we also give the rise of the magnetic field observed for $B_{app}=7.6$ and 4.3 kG, within 0.1 mm from the anode surface ($x\lesssim0.1$ mm), taken from Fig. 6. Because of the uncertainty in B_{app} the magnetic field rise is taken with respect to the average of B_{app} and the magnetic field measured when I is zero, i.e., at $t\simeq150$ ns. The difference between the latter and B_{app} was included in the uncertainties in the data points shown in Fig. 7. It is seen that for both applied fields, the assumption of classical conductivity predicts a rise of the magnetic field at the anode surface that is significantly less than that observed.

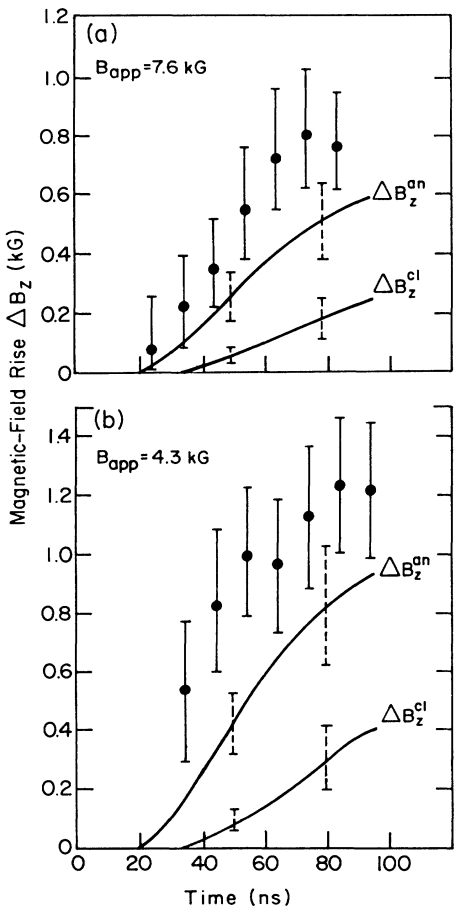

FIG. 7. Calculated magnetic field rise at the anode surface for a classical plasma conductivity that corresponds to $T_e=7$ eV (ΔB_z^{cl}) and for an anomalous conductivity that is ten times lower than the classical conductivity (ΔB_z^{an}) assuming the plasma is 2 mm thick. The uncertainties shown by the dashed error bars include the uncertainties in the ion current density and in the C III fraction in the ion beam. For ΔB_z^{cl}, the uncertainty in the electron temperature (5–8 eV) is also included. Also given is the observed magnetic-field rise within 0.1 mm from the surface taken from Fig. 6. (a) $B_{app}=7.6$ kG, see Fig. 6(a). (b) $B_{app}=4.3$ kG, see Fig. 6(b).

We now assume an anomalous plasma conductivity that is 10× lower than the classical conductivity, as suggested in Ref. 11. The magnetic-field rise ΔB_z^{an} at the anode surface calculated using this conductivity is shown in Fig. 7 for the two applied fields. The calculated magnetic-field rise ΔB_z^{an} is much closer to the observed rise than ΔB_z^{cl}. The difference between the rise of the magnetic field calculated for a classical and an anomalous conductivities and the observed rise is insensitive to the plasma thickness assumed. It is also insensitive to the form of the ion current density $J_i(t)$. Furthermore, if the convective term due to the observed plasma expansion at the rate of $\simeq1$ cm/μs is included in Eq. (4), the difference between ΔB_z^{cl} and the observation would be even larger, while the difference for ΔB_z^{an} would change insignificantly. Thus we may conclude that the observed rise in the magnetic field on the surface is much more consistent with an anomalous plasma conductivity that is ten times lower than the classical conductivity than with a classical conductivity. Plasma conductivities lower than the anomalous conductivity used here are also consistent with the data (see Fig. 7), but for such low values of the conductivity the present measurement is insensitive to the conductivity.

V. SUMMARY

We determined the time-dependent magnetic field in the anode plasma of an intense planar ion beam diode by the observation of line-emission Zeeman splitting. The applied magnetic field was found to be present in the plasma early in the pulse, consistent with a previously suggested mechanism of the plasma formation, based on the ionization of an expanding neutral layer.[14] The magnetic field in the plasma is used to estimate the current density j_y in the plasma resulting from the plasma axial pressure gradient, the electron thermal convection in the plasma, and the Larmor radii of the various plasma ions.[11]

The rise of the magnetic field in the anode plasma due to the electron flow in the diode acceleration gap was also observed. It was found to be much larger than predicted in one-dimensional calculations.[8] However, it is consistent with estimates based on the presently measured ion current density and previous measurements of the electric-field distribution across the diode acceleration

gap in a similar experiment.[10]

The observed penetration of the time-dependent component of the magnetic field into the inner region of the plasma agreed reasonably well with a penetration calculated assuming an anomalous plasma conductivity about 10× lower than the classical conductivity. This anomalous plasma conductivity significantly reduces the currents induced in the plasma by the penetrating magnetic field that tend to push the plasma back to the anode surface. This effect and the increased electron collisionality serves to explain the relatively fast plasma expansion against the magnetic field[11] and the uniformity of the electron temperature across the plasma.[12] Furthermore, together with the currents due to the plasma pressure gradient, it yields an electron Ohmic heating rate that is about balanced by the electron cooling rate in the plasma, which is consistent with the approximate constancy of the electron temperature during the pulse.[12,13]

We believe that the presently developed technique for measuring the magnetic field in the anode plasma of a magnetically insulated ion diode can be employed for plasmas produced in various high-power high-voltage devices. Knowledge of the diamagnetic effects in high-power diodes is important since these effects strongly influence the current flow in the diode gap, as discussed by Miller[18] and Slutz *et al.*[19] They also affect the anode plasma heating and instability.[20,21] Also, in higher-power diodes the stronger magnetic fields induced in the plasma will probably result in a better measurement accuracy due to the larger Zeeman splitting. This will make possible better estimates of the plasma conductivity. Local measurements can be made by "seeding" the anode plasma with the desirable species in limited regions of the plasma, as is done in Ref. 11. Measurements of the diamagnetic effects in the cathode plasma of a device can be made in a similar manner. These can provide additional information about the current flow in the device. Measurements of the magnetic-field time history in plasma opening switches[6,7] are expected to be of great importance for the understanding of the switch operation. Also, in various plasma sources in which the ions are colder than in our plasma smaller magnetic fields can be measured due to the smaller line Doppler broadening. Finally, the use of laser-induced two-photon processes with a geometry previously suggested[22] is expected to allow for measurements of smaller magnetic fields with an improved spatial resolution in all directions.

ACKNOWLEDGMENTS

We are thankful to L. Perelmutter and M. Sarfaty for stimulating discussions and help in the experiments. Valuable comments and critical reading of the manuscript by A. E. Blaugrund and Z. Zinamon are gratefully acknowledged. We thank A. Fisher, C. Litwin, R. N. Sudan, and A. Fructhman for illuminating remarks. The skilled technical assistance of P. Meiri and Y. Danino is appreciated.

[1]See, for example, R. B. Miller, *Intense Charged Particle Beams* (Plenum, New York, 1982), and references therein.

[2]P. Dreike, C. Eichenberger, S. Humphries, and R. N. Sudan, J. Appl. Phys. **47**, 85 (1976); S. Humphries, Jr., Nucl. Fusion **20**, 1549 (1980).

[3]J. P. VanDevender, Plasma Phys. Controlled Fusion **28**, 841 (1986).

[4]T. J. Orzechowski and G. Bekefi, Phys. Fluids **19**, 43 (1976); **22**, 978 (1979).

[5]C. W. Mendel, Jr., D. B. Seidel, and S. E. Rosental, Laser Part. Beams **1**, 311 (1983); C. W. Mendel, Jr., D. B. Seidel, and S. A. Slutz, Phys. Fluids **26**, 3628 (1983).

[6]C. W. Mendel, Jr. and S. A. Goldstein, J. Appl. Phys. **48**, 1004 (1977).

[7]P. Ottinger, S. A. Goldstein, and R. A. Meger, J. Appl. Phys. **56**, 774 (1984).

[8]T. M. Antonsen and E. Ott, Phys. Fluids **19**, 52 (1976).

[9]C. W. Mendel, Jr. and J. P. Quintenz, Comments Plasma Phys. Controlled Fusion **8**, 43 (1983).

[10]Y. Maron, M. D. Coleman, D. A. Hammer, and H. S. Peng, Phys. Rev. A **36**, 2818 (1987).

[11]Y. Maron, E. Sarid, O. Zahavi, L. Perelmutter, and M. Sarfaty, preceding paper, Phys. Rev. A **39**, 5842 (1989).

[12]Y. Maron, M. Sarfaty, L. Perelmutter, O. Zahavi, M. E. Foord, and E. Sarid (unpublished).

[13]Y. Maron, L. Perelmutter, E. Sarid, E. Foord, and M. Sarfaty (unpublished).

[14]C. Litwin and Y. Maron, Phys. Fluids B **1**, 670 (1989).

[15]S. I. Braginskii, in *Reviews of Plasma Physics,* edited by M. A. Leontovich (Consultants Bureau, New York, 1965), Vol. 1, p. 205.

[16]R. V. Lovelace and E. Ott, Phys. Fluids **17**, 1263 (1974); A. W. Hull, Phys. Rev. **18**, 31 (1921).

[17]D. B. Seidel, S. A. Slutz, and C. W. Mendel (private communication).

[18]P. A. Miller, J. Appl. Phys. **57**, 1473 (1985).

[19]S. A. Slutz, D. B. Seidel, and R. S. Coats, J. Appl. Phys. **59**, 11 (1986).

[20]C. L. Olson, Laser Part. Beams **2**, 255 (1984).

[21]S. A. Slutz, J. Appl. Phys. **61**, 1288 (1987).

[22]Y. Maron and C. Litwin, J. Appl. Phys. **54**, 2086 (1983).